Journal of Human Evolution 57 (2009) 191–194

Contents lists available at ScienceDirect

Journal of Human Evolution

journal homepage: www.elsevier.com/locate/jhevol

News and Views

# Computing singular warps from Procrustes aligned coordinates

Kieran P. McNulty

*Department of Anthropology, University of Minnesota, 395 Hubert H. Humphrey Center, 301 19th Avenue South, Minneapolis, MN 55455, USA*

ARTICLE INFO

*Article history:*
Received 6 June 2008
Accepted 25 May 2009

*Keywords:*
Singular warps
Partial least squares
Cross-covariance matrix

Landmark-based morphometric methods enjoy substantial popularity among morphological researchers in biological anthropology (Richtsmeier et al., 2002), and in some respects were developed and established within the broader community of evolutionary anthropologists and biologists (see Bookstein et al., 2004; Slice, 2007). Beyond the basic tools for analyzing landmark data—Procrustes superimposition, thin-plate splines—one of the most exciting methods to emerge from the geometric morphometric school is the application of partial least squares analysis to shape data (Rohlf and Corti, 2000; Bookstein et al., 2003). Using this approach, researchers are now able to specifically examine complex patterns of covariation between multiple sets of variables, addressing such critical issues as morphological integration (e.g., Bookstein et al., 2003; Bastir and Rosas, 2005; Bastir et al., 2005; Mitteroecker and Bookstein, 2007, 2008), ecomorphology (Corti et al., 1996), phylogeography (Fadda and Corti, 1998; Frost et al., 2003; Rosas et al., 2006), and even morphological homology (e.g., Gunz and Harvati, 2007). When one set of these variables consists of shape coordinates, the analysis is considered a specific type of partial least squares called singular warps analysis (Bookstein et al., 2003).

In its simplest manifestation, a comparison between two blocks of data or two-block partial least squares, singular warps analysis is based on a singular value decomposition of the cross-covariance matrix of two sets of variables measured from the same sample of objects (Rohlf and Corti, 2000; Bookstein et al., 2003). Unlike a typical covariance matrix, the cross-covariance matrix describes how each variable in one set covaries with each variable in another, without including covariances between variables *within* either set. It may be more intuitively understood as a submatrix of the usual covariance matrix, which contains only the covariances between the two sets of variables. For example, a covariance matrix for six variables ($y_1$–$y_6$) contains the variance of each on the diagonal and covariances between every pair of variables in off-diagonal cells (Fig. 1). If, however, these six measurements are instead conceived of as belonging to two sets of variables, Y1 = {$y_1$, $y_2$} and Y2 = {$y_3$, $y_4$, $y_5$, $y_6$}, the cross-covariance matrix is simply the off-diagonal block of covariances that compares variables in Y1 with those in Y2 (Fig. 1, shaded in grey). A singular value decomposition of this cross-covariance matrix, then, provides a method for exploring covariation between the two sets of variables rather than covariation among all of the variables (Rohlf and Corti, 2000).

Accordingly, covariance values in the cross-covariance matrix are not computationally different from those in a typical covariance matrix, and can be calculated from the basic equation for the sample estimate of covariance between two variables ($X$ and $Y$):

$$\mathrm{cov}(X,Y) = \sum_{i=1}^{N} \frac{(x_i - \bar{x})(y_i - \bar{y})}{N-1}, \quad (1)$$

where $N$ is the sample size and $\bar{x}$ and $\bar{y}$ are the arithmetic means of the two variables under consideration. In the initial exposition of singular warps analysis, Bookstein et al. (2003) gave a shortcut equation for computing the cross-covariance matrix that is useful particularly for those researchers who wish to program their own singular warps analyses. This equation bypasses calculation of the full covariance matrix, instead producing only the cross-covariance matrix $\Sigma$:

$$\Sigma = (1/N)X^tY, \quad (2)$$

where $N$ is the sample size and $X$ and $Y$ are matrices for two sets of variables with $N$ rows, corresponding to the same sample of specimens, and columns according to the number of variables in each set. If each variable in both matrices is first mean-centered (by variable), then Equation (2) yields the cross-covariance matrix between variables in $X$ and those in $Y$.

This equation for the cross-covariance matrix (Bookstein et al., 2003; Equation (2) in this paper) provides researchers with the means to adapt singular warps analysis to suit a variety of objectives, some of which may not be possible using readily available partial least squares software packages (e.g., *tpsPLS*, *MorphoJ*, *PAST*, *IMP*). In this case, programmable software packages, such as *R*, *SAS*, or *Matlab*, can be used to compute the analysis directly while offering the flexibility to run it in multiple contexts (e.g., iterated through different sets of variables, exploring the effects of different

*E-mail address:* kmcnulty@umn.edu

0047-2484/$ – see front matter 
doi:10.1016/j.jhevol.2009.05.008

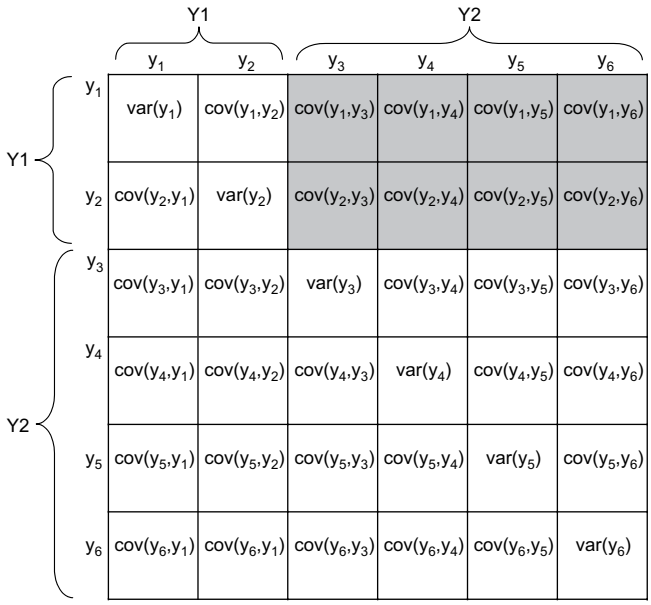


**Figure 1.** Example of a covariance matrix for a dataset with six variables ($y_1$, $y_2$, $y_3$, $y_4$, $y_5$, $y_6$). Variances for each are given on the diagonal of the matrix while covariances between variables are given off the diagonal. If these variables are consigned to two sets, Y1 = {$y_1$, $y_2$} and Y2 = {$y_3$, $y_4$, $y_5$, $y_6$}, the cross-covariance matrix, shaded in grey, is a submatrix of the overall covariance matrix that includes only covariances between a variable in Y1 and a variable in Y2.

superimpositions, computing three-block analyses). Herein lies a potential problem for researchers who are used to performing statistical analyses on Procrustes aligned shape coordinates (or any type of data that are not mean-centered by variable): if entered directly into Equation (2), Procrustes aligned coordinates will not yield a cross-covariance matrix.

It is commonplace in landmark-based morphometric studies to use aligned shape coordinates, either in shape space or tangent space, as variables for analysis (e.g., Singleton, 2002; Frost et al., 2003; Harvati et al., 2004; Lockwood et al., 2004; McNulty, 2004, 2005; McNulty et al., 2006; Cobb and O'Higgins, 2007; Erwin et al., 2007; Baab, 2008; Bruner, 2008; Cardini and Elton, 2008a,b; Kimmerle et al., 2008). Indeed, aligned coordinates are standard output from those software packages most frequently used to perform generalized Procrustes analysis (GPA) (*Morpheus et al.*, Slice, 1998; *tpsSmall*, Rohlf, 2003; *Morphologika*$^2$, O'Higgins and Jones, 2006). However, whereas GPA mean-centers all specimen *configurations*—it superimposes the centroids of each specimen—GPA does not mean-center each coordinate within the specimens, and therefore does not in itself provide suitable variables for use in Equation (2). Because covariance is calculated by mean-centering each variable, i.e., $(x_i - \bar{x})$ and $(y_i - \bar{y})$, entering Procrustes aligned shape coordinates into Equation (2) will not yield a cross-covariance matrix but rather a cross-products matrix. Results of a singular warps analysis computed from a cross-products matrix instead of a cross-covariance matrix may be uninterpretable within the original context of the research question.

Bookstein et al. (2003) properly avoided this problem by computing singular warps from the Procrustes residuals, which are the aligned coordinates mean-centered on their corresponding landmarks in the consensus configuration (Dryden and Mardia, 1998). Mean-centering one's data is necessary in the computation of singular warps, regardless of whether shape space or tangent space coordinates are being used. However, because this step is not specified in the original publication, though implied by the zero-centered singular warps plots, there is a significant chance that some researchers will mistakenly compute $\Sigma$ from Procrustes aligned coordinates rather than from Procrustes residuals. In fact, there is at least one example of this in the literature already (Harcourt-Smith et al., 2008), and the stature of these researchers suggests that this misunderstanding may be easily repeated by other workers.

## Example

A simple example illustrates how one's results might differ if singular warps are mistakenly computed from simple aligned coordinates rather than from mean-centered aligned coordinates. Note that this is only one example, and the specific impact of not mean-centering the data will differ for each dataset. This example is based on 3D cranial landmarks from a sample of twenty *Gorilla gorilla* and twenty *Pan troglodytes* specimens, both evenly divided between sexes. Landmarks were separated into two blocks of data: block 1 comprised "facial" landmarks (R/L mid-torus superior, R/L zygomaxillare, glabella, rhinion, anterior attachment of the nasal septum, alveolare, R/L distal third molar), and block 2 "neurocranial" landmarks (opisthocranion, R/L porion, bregma, basion, hormion). Details about the dataset as well as the coordinate data for these specimens are available at http://anthropologylabs.umn.edu/eal/sas/SASRoutines.phpunde rthe 2BPLS_SW routine. Additional sample descriptions are presented in McNulty (2003). Blocks 1 and 2 were separately superimposed by GPA so as to not introduce covariation due to their relative positions in the cranium. Equation (2) above was used to compute the matrix $\Sigma$ from both non-mean-centered and mean-centered aligned coordinates ($X$ = block 1 variables, $Y$ = block 2 variables). Singular value decompositions were then performed on both $\Sigma$s, and $X$ and $Y$ were matrix multiplied by their corresponding singular vector matrices to obtain scores for each specimen on the singular warps.

Results of the two analyses are summarized in Fig. 2 as plots of the first singular warps for the neurocranial versus the facial landmarks. The left graph (Fig. 2a) illustrates specimen scores obtained without mean-centering the data, while the right graph (Fig. 2b) shows singular warp scores from mean-centered aligned coordinates. One can see a clear difference in the pattern of specimen distributions along the eigenvectors in these graphs, and, in fact, even the direction of the correlations between the two blocks is different. This demonstrates that interpretations of these results—e.g., the degree of covariance between data blocks, specific landmarks that covary the most, shape changes associated with the covariance pattern—would differ greatly. Calculating the angles between the two block 1 vectors (facial landmarks) and between the two block 2 vectors (neurocranial landmarks) showed both cases to be nearly orthogonal (>85°), indicating that these vectors capture very different aspects of shape change. Results from the mean-centered data (Fig. 2b) are also more interpretable, with distinct taxon clusters and, among gorillas, separation of males and females along the properly computed singular warps. Finally, one can see that the mean-centered data produce scores that themselves are mean-centered (i.e., the centroid of the scatter is 0,0), although this follows specifically from multiplying the singular vectors by mean-centered data, and not necessarily from centering data to compute the cross-covariance matrix.

## Computing singular warps

Many practitioners of geometric morphometrics will find that available software packages for computing two-block partial least squares analyses are sufficient for their research needs and will thereby avoid the problem outlined here. Freely available programs that perform these computations include *tpsPLS* (Rohlf, 2006), *MorphoJ* (Klingenberg, 2008), *PAST* (Hammer et al., 2001), and

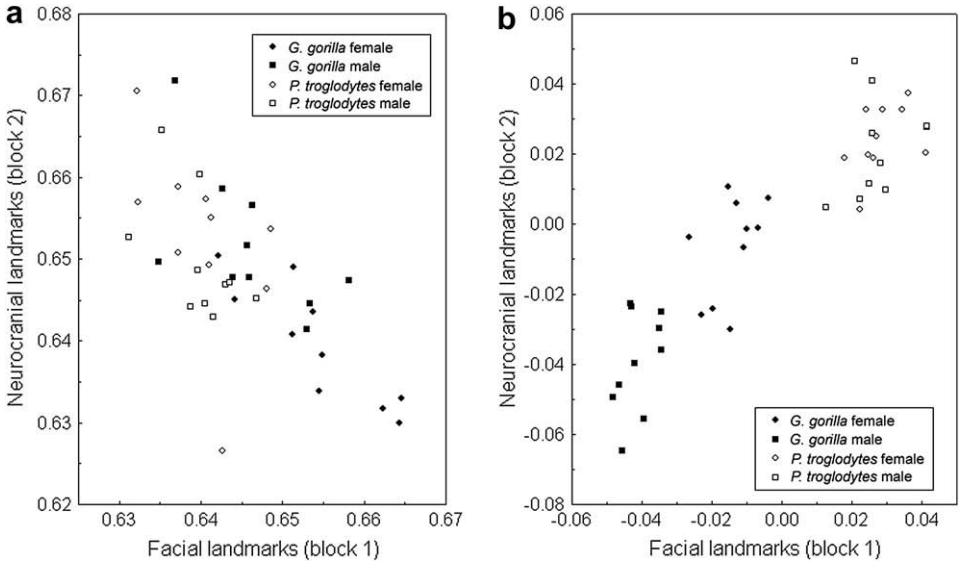


**Figure 2.** Plot of specimen scores on the first singular vectors of the matrix Σ, which was computed from Equation (2) using (a) Procrustes aligned shape coordinates, and (b) mean-centered aligned coordinates (Procrustes residuals). In this example, the data are 3D cranial landmarks from a sample of *Gorilla gorilla* and *Pan troglodytes*, with facial landmarks (block 1) represented by scores on the x-axis and neurocranial landmarks (block 2) by scores on the y-axis. When mean-centered data are used in Equation 2 (b), Σ represents the cross-covariance matrix between the two blocks of data and its singular value decomposition results in singular warps that summarize covariation between those blocks.

components of the *IMP* software series (Sheets, 2004). However, researchers who require the greater flexibility afforded by programmable statistical packages will need to convert their aligned coordinates into Procrustes residuals by mean-centering them before computing a cross-covariance matrix. Of the most frequently used superimposition programs, only *PAST* (Hammer et al., 2001) provides an option for outputting Procrustes residuals. Any program that performs a generalized Procrustes analysis (e.g., *Morpheus et al.*, *tpsSmall*, *Morphologika*$^2$, *MorphoJ*), however, will also generate mean configurations, and these can be easily subtracted from the aligned coordinates to mean-center the data. One could do this automatically in programmable statistical packages using simple scripts, or manually in any spreadsheet program. As a final alternative, some researchers might consider generating a standard covariance matrix using pre-programmed statistical modules (e.g., principal components analysis) and then extracting only those rows and columns of the matrix that correspond to the cross-block covariances (see Fig. 1).

To conclude, the singular warps approach fully developed in Bookstein et al. (2003) fills an important gap in the toolkit for understanding and quantifying biological relationships (Bookstein and Rohlf, 2004). Moreover, Bookstein and colleagues (2003; Gunz and Harvati, 2007; Mitteroecker and Bookstein, 2007, 2008) provide a methodological clarity often absent from morphometric literature, thereby enabling other researchers to apprehend and utilize this important new approach. Nevertheless, with the growing popularity of geometric morphometrics and the wide availability of programmable statistical software, there is a real chance for this particular equation to be misapplied by workers who typically rely on aligned coordinates for their analyses. It is hoped that this note will prevent such misunderstandings in the computation of singular warps and aid researchers in obtaining robust and interpretable results.

## Acknowledgements

I thank Steve Frost, Tim Weaver, and Will Harcourt-Smith for encouraging me to write this and for their thoughtful comments on this note. In addition, Dennis Slice and Fred Bookstein helped me to clarify several points herein. I am especially grateful to Jim Rohlf for his thorough and insightful remarks on an early draft, and thank the editor, associate editor, Markus Bastir, and one anonymous reviewer for their constructive and critical feedback. This paper is NYCEP Morphometrics Contribution #38.

## References

Baab, K.L., 2008. The taxonomic implications of cranial shape variation in *Homo erectus*. J. Hum. Evol. 54, 827–847.
Bastir, M., Rosas, A., 2005. Hierarchical nature of morphological integration and modularity in the human posterior face. Am. J. Phys. Anthropol. 128, 26–34.
Bastir, M., Rosas, A., Sheets, D.H., 2005. The morphological integration of the hominoid skull: a partial least squares and PC analysis with morphogenetic implications for European Mid-Pleistocene mandibles. In: Slice, D. (Ed.), Modern Morphometrics in Physical Anthropology. Kluwer Academic/Plenum Publishers, New York, pp. 265–284.
Bookstein, F.L., Rohlf, F.J., 2004. From "mathematical dissection of anatomies" to morphometrics: a twenty-first century appreciation of Charles Oxnard. In: Anapol, F., German, R.Z., Jablonski, N.G. (Eds.), Shaping Primate Evolution. Cambridge University Press, Cambridge, pp. 378–390.
Bookstein, F.L., Gunz, P., Mitteroecker, P., Prossinger, H., Shaefer, K., Seidler, H., 2003. Cranial integration in *Homo*: singular warps analysis of the midsagittal plane in ontogeny and evolution. J. Hum. Evol. 44, 167–187.
Bookstein, F.L., Slice, D.E., Gunz, P., Mitteroecker, P., 2004. Anthropology takes control of morphometrics. Coll. Antropol. 28 (Suppl. 2), 121–132.
Bruner, E., 2008. Comparing endocranial form and shape differences in modern humans and Neandertals: a geometric approach. PaleoAnthropology 2008, 93–106.
Cardini, A., Elton, S., 2008a. Variation in guenon skulls (I): species divergence, ecological and genetic differences. J. Hum. Evol. 54, 615–637.
Cardini, A., Elton, S., 2008b. Variation in guenon skulls (II): sexual dimorphism. J. Hum. Evol. 54, 638–647.
Cobb, S.N., O'Higgins, P., 2007. The ontogeny of sexual dimorphism in the facial skeleton of the African apes. J. Hum. Evol. 53, 176–190.
Corti, M., Fadda, C., Simson, S., Nevo, E., 1996. Size and shape variation in the mandible of the fossorial rodent *Spalax ehrenbergi*. In: Marcus, L.F., Corti, M., Loy, A., Naylor, G.J.P., Slice, D.E. (Eds.), Advances in Morphometrics. NATO ASI Ser, 284, pp. 303–320.
Dryden, I.L., Mardia, K.V., 1998. Statistical Shape Analysis. John Wiley & Sons, New York.
Erwin, J., Prossinger, H., Bookstein, F.L., Schaefer, K., Bernhard, M., Freudenthalere, J.W., 2007. Secular trends in the facial skull from the 19th century to the present, analyzed with geometric morphometrics. Am. J. Orthod. Dentofacial Orthop. 132, 63–70.
Fadda, C., Corti, M., 1998. Geographic variation of *Arvicanthis* (Rodentia, Muridae) in the Nile Valley. Z. Säugetierk 63, 104–113.
Frost, S.R., Marcus, L.F., Bookstein, F.L., Reddy, D.P., Delson, E., 2003. Cranial allometry, phylogeography, and systematics of large-bodied papionins

(Primates: Cercopithecinae) inferred from geometric morphometric analysis of landmark data. Part A. Anat. Rec. 275A, 1048–1072.
Gunz, P., Harvati, K., 2007. The Neanderthal "chignon": variation, integration, and homology. J. Hum. Evol. 52, 262–274.
Hammer, Ø., Harper, D.A.T., Ryan, P.D., 2001. PAST: palaeontological statistics software package for education and data analysis. Palaeontologia Electronica 4, 9 pp. v. 1.90 downloaded from. http://folk.uio.no/ohammer/past/.
Harcourt-Smith, W.E.H., Tallman, M., Frost, S.R., Wiley, D.F., Rohlf, F.J., Delson, E., 2008. Analysis of selected hominoid joint surfaces using laser scanning and geometric morphometrics: a preliminary report. In: Sargis, E.J., Dagosto, M. (Eds.), Mammalian Evolutionary Morphology: A Tribute to Frederick S. Szalay. Springer, New York, pp. 373–383.
Harvati, K., Frost, S.R., McNulty, K.P., 2004. Neanderthal taxonomy reconsidered: implications of 3D primate models of intra- and interspecific differences. Proc. Natl. Acad. Sci. U. S. A. 101, 1147–1152.
Kimmerle, E.H., Ross, A., Slice, D.E., 2008. Sexual dimorphism in America: geometric morphometric analysis of the craniofacial region. J. For. Sci. 53, 54–57.
Klingenberg, C.P., 2008. MorphoJ software. Faculty of Life Sciences, University of Manchester. Available from: http://www.flywings.org.uk/MorphoJ_page.htm.
Lockwood, C.A., Kimbel, W.H., Lynch, J.M., 2004. Morphometrics and hominoid phylogeny: support for a chimpanzee–human clade and differentiation among great ape subspecies. Proc. Natl. Acad. Sci. U. S. A. 101, 4356–4360.
McNulty, K.P., 2003. Geometric morphometric analyses of extant and fossil hominoid craniofacial morphology. Ph.D. Dissertation, City University of New York.
McNulty, K.P., 2004. A geometric morphometric assessment of hominoid crania: conservative African apes and their liberal implications. Ann. Anat. 186, 429–433.
McNulty, K.P., 2005. A geometric morphometric assessment of the hominoid supraorbital region: affinities of the Eurasian Miocene hominoids *Dryopithecus, Graecopithecus, and Sivapithecus*. In: Slice, D. (Ed.), Modern Morphometrics in Physical Anthropology. Kluwer Academic/Plenum Publishers, New York, pp. 349–373.
McNulty, K.P., Frost, S.R., Strait, D.S., 2006. Examining affinities of the Taung child by developmental simulation. J. Hum. Evol. 51, 274–296.
Mitteroecker, P., Bookstein, F.L., 2007. The conceptual and statistical relationship between modularity and morphological integration. Syst. Biol. 56, 818–836.
Mitteroecker, P., Bookstein, F.L., 2008. The evolutionary role of modularity and integration in the hominoid cranium. Evolution 62, 943–958.
O'Higgins, P., Jones, N., 2006. HYMS functional morphology and evolution. Available online at: http://www.york.ac.uk/res/fme/resources/software.htm.
Richtsmeier, J.T., Deleon, V.B., Lele, S.R., 2002. The promise of geometric morphometrics. Yrbk. Phys. Anthropol. 45, 63–91.
Rohlf, F.J., 2003. tpsSmall. v1.20. Department of Ecology, State University of New York, Stony Brook, New York.
Rohlf, F.J., 2006. tpsPLS. v1.18. Department of Ecology, State University of New York, Stony Brook, New York.
Rohlf, F.J., Corti, M., 2000. Use of two-block partial least-squares to study covariation in shape. Syst. Biol. 49, 740–753.
Rosas, A., Martínez-Mazaa, C., Bastir, M., García-Taberneroa, A., Lalueza-Fox, C., Huguet, R., Eugenio Ortiz, J., Julià, R., Soler, V., de Torres, T., Martínez, E., Cañaveras, J.C., Sánchez-Moral, S., Cuezva, S., Lariol, J., Santamaría, D., de la Rasilla, M., Fortea, J., 2006. Paleobiology and comparative morphology of a late Neandertal sample from El Sidrón, Asturias, Spain. Proc. Natl. Acad. Sci. U. S. A. 103, 19266–19271.
Sheets, H.D., 2004. IMP-integrated Morphometrics Package. Department of Physics, Canisius College, New York. Available from: http://www.canisius.edu/~sheets/morphsoft.html.
Singleton, M., 2002. Patterns of cranial shape variation in the Papionini (Primates: Cercopithecinae). J. Hum. Evol. 42, 547–578.
Slice, D.E., 1998. Morpheusx et al. Software for Morphometric Research. Department of Ecology, State University of New York, Stony Brook, New York.
Slice, D.E., 2007. Geometric morphometrics. Annu. Rev. Anthropol. 36, 261–281.